Kelemen, P.B., Kikawa, E., and Miller, D.J. (Eds.)
Proceedings of the Ocean Drilling Program, Scientific Results Volume 209

4. Hybridization of Dunite and Gabbroic Materials in Hole 1271B from Mid-Atlantic Ridge 15°N: Implications for Melt Flow and Reaction in the Upper Mantle[1]

Eiichi Takazawa,[2] Natsue Abe,[3] Monique Seyler,[4] and William P. Meurer[5]

ABSTRACT

Dunite and gabbroic materials recovered from Hole 1271B, Ocean Drilling Program (ODP) Leg 209, were examined for mineral chemistry to understand melt flow and melt-mantle reactions in the shallowest upper mantle of the Mid-Atlantic Ridge near the 15°20′ Fracture Zone. Hole 1271B was drilled to 103.8 meters below seafloor on the inner corner high along the south wall of the 15°20′ Fracture Zone. The total length of core collected was 15.9 m (recovery = ~15%). The dominant rock type in Hole 1271B is dunite, followed by brown amphibole gabbro, olivine gabbro, and troctolite, along with minor amounts of harzburgite and olivine gabbronorite. A large proportion of the dunite is associated with gabbroic rocks in Hole 1271B, similar to those observed in the Mohorovicic (Moho) transition zone of the Oman ophiolite, indicating significant magmatic activity in this region near the 15°20′ Fracture Zone. Olivine Fo content varies from 89.2 to 91.2 in impregnated dunite and from 85.6 to 88.6 in troctolite, olivine gabbro, and olivine gabbronorite. Spinel Cr# (= 100 × Cr/[Cr + Al] molar ratio) ranges from 38.9 to 62.7 in dunite and from 46.3 to 57.6 in troctolites, olivine gabbro, and olivine gabbronorite. Compositional trends for spinel from dunite through troctolite toward olivine gabbro/gabbronorite are characterized by increases in TiO_2, Cr#, and Fe^{3+}#, very

[1]Takazawa, E., Abe, N., Seyler, M., and Meurer, W.P., 2007. Hybridization of dunite and gabbroic materials in Hole 1271B from Mid-Atlantic Ridge 15°N: implications for melt flow and reaction in the upper mantle. *In* Kelemen, P.B., Kikawa, E., and Miller, D.J. (Eds.), *Proc. ODP, Sci. Results,* 209: College Station, TX (Ocean Drilling Program), 1–23. doi:10.2973/odp.proc.sr.209.005.2007
[2]Department of Geology, Faculty of Science, Niigata University, 2-8050 Ikarashi, Nishi-ku, Niigata, 950-2181, Japan. **takazawa@geo.sc.niigata-u.ac.jp**
[3]Deep Sea Research Department, Japan Agency for Marine-Earth Science and Technology, 2-15 Natsushima-cho, Yokosuka 237-0061, Japan.
[4]Museum National d'Histoire Naturelle, CNRS UMR 7160 Minéralogie-Pétrologie, 61 rue Buffon, 75005 Paris, France.
[5]Department of Geosciences, University of Houston, 312 Science and Research Building 1, Houston TX 77204-5007, USA.

Initial receipt: 5 February 2007
Acceptance: 5 June 2007
Web publication: 3 July 2007
Ms 209SR-005

similar to those reported from Hess Deep Site 895. Olivine gabbro, olivine gabbronorite, and troctolite in Hole 1271B are considered to have formed as hybrid rocks between dunite and an evolved melt in the walls of a melt channel in the shallowest upper mantle that is tens of meters wide. The melt trapped in the wall rock crystallized plagioclase and clinopyroxene. On the other hand, dunite in the center of the melt channel became more refractory by melt-mantle reactions, increasing spinel Cr# to 62.5.

INTRODUCTION

Abyssal peridotites are exposed in the regions of ridge segmentation with reduced crustal thickness at slow spreading ridges (Dick, 1989; Cannat et al., 1995; Cannat, 1996). During Ocean Drilling Program (ODP) Leg 209, mantle peridotites exposed on the seafloor at the Mid-Atlantic Ridge from 14° to 16°N near the 15°20′ Fracture Zone were drilled. The primary aim of drilling was to characterize the spatial variation of mantle deformation patterns, residual peridotite composition, melt migration features, plutonic rocks, and hydrothermal alteration along axis (Kelemen, Kikawa, Miller, et al., 2004). Peridotite cores recovered during this leg were serpentinized harzburgite and dunite associated with gabbroic intrusion. Many residual peridotites indicate textural features of interaction with melt migrating along grain boundaries by diffused porous flow at the base of the thermal boundary layer (Seyler et al., 2007), whereas the presence of impregnated peridotites and hybrid troctolites at Sites 1271 and 1275 suggest extensive crystallization of intergranular melt at lower temperatures (Kelemen, Kikawa, Miller, et al., 2004). In this paper, we report chemical compositions for primary minerals in altered dunites and associated plutonic rocks recovered from Hole 1271B and discuss melt flow and reaction in the shallow upper mantle at the Mid-Atlantic Ridge near the 15°20′ Fracture Zone.

HOLE 1271B STRATIGRAPHY

Hole 1271B was drilled to 103.8 meters below seafloor (mbsf) on the inner corner high along the south wall of the 15°20′ Fracture Zone (Fig. F1). The total length of core collected was 15.9 m (recovery = ~15%). Recovered cores are so severely altered so that primary lithology was estimated from assemblages of relict and alteration minerals. Spinel remains as a relict mineral in peridotite, although olivine and orthopyroxene are replaced by serpentine. In Hole 1271B, dunite is dominant (56%) followed by brown amphibole gabbro (21%) and olivine gabbro and troctolite (14%). Harzburgite occupies <1% in Hole 1271B. The large amount of dunite in Hole 1271B differs from the other holes drilled near the 15°20′ Fracture Zone, where harzburgite and gabbroic plutonic rocks are more dominant.

The cores in Hole 1271B are divided into four units on the basis of rock type variation (Fig. F2) (Kelemen, Kikawa, Miller, et al., 2004). Units I, II, and IV mainly consist of dunite and brown amphibole gabbro with minor amounts of harzburgite and chromitite, whereas Unit III consists of olivine gabbro, troctolite, dunite, and brown amphibole gabbro. Olivine gabbro and troctolite dominate in the upper and lower horizon of Unit III. In contrast, brown amphibole gabbro is present through all Hole 1271B units. A small chromitite pod enclosed in

F1. Leg 209 drilling sites, p. 10.

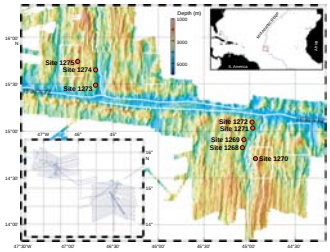

F2. Lithostratigraphic summary, Hole 1271B, p. 11.

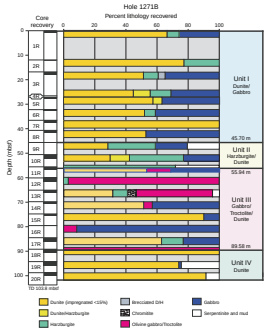

spinel-rich dunite was recovered from Unit III (interval 209-1271B-13R-1, 32–38 cm).

PETROGRAPHY

All the samples examined in this study were collected from Hole 1271B. Hydrothermal alteration of recovered cores from Hole 1271B was fully described in the Leg 209 *Initial Reports* volume (Kelemen, Kikawa, Miller, et al., 2004). Principal features are described for each lithology below.

Dunite and Harzburgite

Dunite and harzburgite in Hole 1271B are heavily altered. Olivine is completely replaced by serpentine and magnetite, whereas orthopyoxene is altered to bastite pseudomorphs. Reddish brown spinel of rounded shape is present in most samples that have survived alteration. Pseudomorphs after olivine and orthopyroxene are recognized by shape because magnetites frequently form trails along grain boundaries of these pseudomorphs. On the basis of magnetite trails, the primary texture of dunite is inferred to be equigranular. Some dunites in Units II–IV contain veinlets and patches composed of fine-grained talc, chlorite, and amphibole along grain boundaries. We interpret this alteration phase as hydrothermal alteration of plagioclase and clinopyroxene crystallized from melts migrating along grain boundaries in dunite (Kelemen, Kikawa, Miller, et al., 2004). Here we call dunite with interstitial gabbroic material "impregnated dunite."

The shape and size of spinel grains in dunite vary with location in Hole 1271B (Fig. F3). The size of spinel grains decreases from Unit I to Unit III. Dunite in Unit I contains spinel grains 1–2 mm in size. Only a few grains occur in one thin section. Spinel grains in impregnated dunite in Unit II are much smaller (<1 mm) and form symplectite with amphibole on the rims. Unit III dunites contain a large number of spinel grains with smaller euhedral shape (<0.5 mm).

F3. Spinel grains, p. 12.

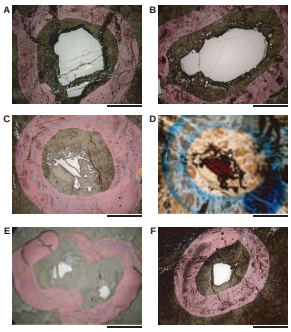

Troctolite, Olivine Gabbro, and Olivine Gabbronorite

Varying amounts of gabbroic material within the dunite matrix cause various lithologies in Hole 1271B, such as troctolite, olivine gabbro, and olivine gabbronorite. Gabbroic material in impregnated dunite is present along olivine grain boundaries and/or forms disaggregate olivine matrix in centimeter-sized fragments. Gabbroic materials also fill microfractures crosscutting the olivine matrix. Alteration also severely affects gabbroic materials; only olivine and spinel are relict minerals in these rocks, whereas gabbroic materials are replaced by hornblendic amphibole, tremolite-actinolite, talc, chlorite, sericite, metamorphic plagioclase, and minor quartz. On the basis of proportion of primary and alteration minerals, we inferred the primary lithologies and classified them into troctolite, olivine gabbro, and olivine gabbronorite. Gabbroic materials are interpreted as crystallization products of melt migrating through peridotite (Kelemen, Kikawa, Miller, et al., 2004). The amount of gabbroic materials increases in the following order: impregnated dunite, troctolite, and olivine gabbro/gabbronorite.

Brown Amphibole Gabbro

Brown amphibole gabbro consists of brown amphibole and plagioclase with minor amounts of ilmenite, rutile, titanite, and zircon. This rock type is distinguished from olivine gabbro by the presence of brown amphibole and the absence of olivine. Brown amphiboles are partially altered to low-temperature amphiboles such as tremolite. Plagioclases mostly become sericite except for a few grains.

MINERAL CHEMISTRY

Major element compositions of primary minerals (olivine, spinel, and amphibole) were determined using an electron probe microanalyzer with wavelength dispersive X-ray spectrometry (JEOL JXA-8600SX) at Niigata University (Japan). Operating conditions were 15-kV accelerating voltage, 13-nA beam current, and ~1-µm beam diameter, using the oxide ZAF (atomic number, absorption, and fluorescence) matrix correction program. Averaged major element compositions for olivine, spinel, and amphibole in selected samples are listed in Tables T1, T2, and T3.

Olivine

Olivine crystals that escaped serpentinization occur in olivine gabbro, olivine gabbronorite, troctolite, and impregnated dunite. Fo content of the olivine crystals varies from 89.2 to 91.2 in an impregnated dunite (Sample 209-1271B-10R-1, 43–46 cm) that is more Fe rich than harzburgites from Holes 1272A and 1274A (Fig. F4). Fo content of olivine in troctolite, olivine gabbro, and olivine gabbronorite is much lower and varies from 85.6 to 88.6.

Spinel

Spinel occurs in most rocks. Cr# of spinel (= 100 × Cr/[Cr + Al] molar ratio) ranges from 38.9 to 62.7 in dunites, 46.9 to 59.1 in impregnated dunites, and 46.3 to 57.6 in troctolites, olivine gabbros, and olivine gabbronorite (Table T2). Spinel in a harzburgite (Sample 209-1271B-5R-1, 64–67 cm) has the lowest Cr# of 37.4 ± 0.5. Mg# of spinel (= 100 × Mg/[Mg + Fe^{2+}] molar ratio) negatively correlates with Cr# (Fig. F5). Spinels in dunites lay at the extreme Cr rich end of the range for abyssal peridotites (Dick and Bullen, 1984). Spinels in troctolites, olivine gabbros, and olivine gabbronorite tend to have lower Mg#s than those in dunites, impregnated dunites, and harzburgite.

In Figures F6 and F7, spinel TiO_2 content positively correlates with Cr# and Fe^{3+}# (= Fe^{3+}/[Cr + Al + Fe^{3+}] molar ratio) from dunite through troctolite toward olivine gabbro/gabbronorite, whereas some high-Cr# spinels in dunites and troctolites from Unit III have extremely low TiO_2 and Fe^{3+}#. The former variation is very similar to spinels in peridotites and plutonic intrusions from Hess Deep Site 895 (Arai and Matsukage, 1996; Dick and Natland, 1996).

Figure F8 shows the relationship between Fo content of olivine and Cr# of spinel for Hole 1271B in comparison with harzburgites from Holes 1272A and 1274A and a general trend for mantle peridotite (i.e., the olivine-spinel mantle array proposed by Arai, 1994). Olivine and spinel from troctolite, olivine gabbro, and olivine gabbronorite are plot-

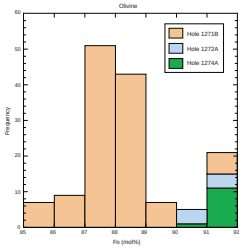

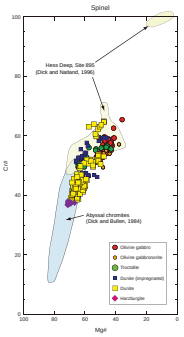

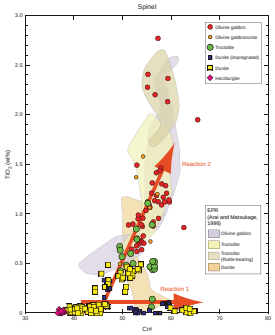

ted out of the olivine-spinel mantle array, with lower Fo contents relative to the impregnated dunite in Unit II and harzburgites from Holes 1272A and 1274A. The compositional ranges for troctolite, olivine gabbro, and olivine gabbronorite coincide with those from Hess Deep Site 895 (Arai and Matsukage, 1996). A dunite (Sample 209-1271B-10R-1, 43–46 cm) from Hole 1271B has olivine with higher Fo content than others and plots inside the olivine-spinel mantle array, similar to harzburgites from other holes.

Amphibole

Amphiboles in Hole 1271B peridotite and plutonic rocks are mostly edenitic in composition, spanning between tremolite and pargasite end-members (Fig. F9). Amphiboles in dunite, troctolite, and olivine gabbro are characterized by lower TiO_2 (0.04–0.7 wt%) and higher Cr_2O_3 (0.3–2.4 wt%) contents, in contrast to those in brown amphibole gabbros with higher TiO_2 (1.4–2.7 wt%) and lower Cr_2O_3 (<0.05 wt%). Mg# of amphibole ranges 0.92 in dunite, 0.91–0.92 in troctolite, 0.88–0.90 in olivine gabbro, and 0.83–0.90 in brown amphibole gabbro.

Downhole Variation of Mineral Composition

Figure F10 shows the downhole compositional variation of olivine and spinel in Hole 1271B. Mineral compositions vary systematically as a function of depth and lithology. The Fo content of olivine decreases from Unit II toward the center of Unit III, whereas Cr# of spinel increases from Unit I to Unit III with a maximum in the center of Unit III. Cr# of spinel from the dunite in Unit III is greater than those in Units I and IV. TiO_2 weight percent and Fe^{3+}# of spinel vary widely with lithology and stratigraphic position. Spinels in harzburgite, dunites, and impregnated dunites in Units I and II have low TiO_2 contents, <0.05 wt% (Fig. F11). In Unit III spinel, TiO_2 contents vary from 0.02 to 0.40 wt% for dunite and impregnated dunite, 0.34 to 0.69 wt% for troctolites, and 0.68 to 2.29 wt% for olivine gabbros and olivine gabbronorite. TiO_2 weight percent and Fe^{3+}# of spinel significantly increase in the upper and lower parts of Unit III, where olivine gabbro, olivine gabbronorite, and troctolite are present. It should be noted that both downhole lithological and compositional variations are symmetric, with a center axis at the Unit III dunite horizon.

DISCUSSION

A large volume of dunite (56%) associated with a minor amount of harzburgite (<1%) is a peculiar characteristic of Hole 1271B relative to other holes, where dunite constitutes 5%–20% of recovered cores, except for Hole 1271A (98%). Dunite in abyssal peridotite and ophiolite has been considered to be a reaction product of harzburgite and orthopyroxene-undersaturated mid-ocean-ridge basalt (MORB) melt that dissolved orthopyroxene during melt migration in the shallow upper mantle (Quick, 1981; Kelemen, 1990; Kelemen et al., 1997). The large volume of dunite at Site 1271 indicates abundant melt migration and reaction in this region. Because of low Mg# and Ni content in whole rock, Kelemen, Kikawa, Miller, et al. (2004) concluded that the Site 1271 dunites are the product of combined olivine crystallization and reaction between residual peridotite and migrating melts with relatively

F7. TiO_2 vs. Fe# for spinel, Hole 1271B, p. 16.

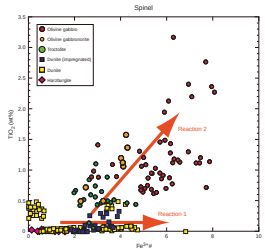

F8. Cr# of spinel vs. Fo of olivine, Holes 1271B, 1272A, and 1274A, p. 17.

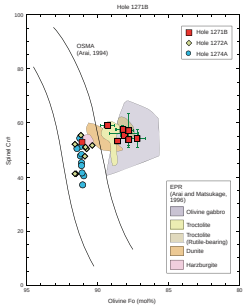

F9. Ca amphibole compositions plotted on Na + K vs. Si, p. 18.

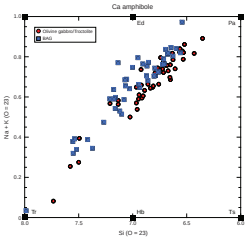

F10. Compositional variations of olivine and spinel, p. 19.

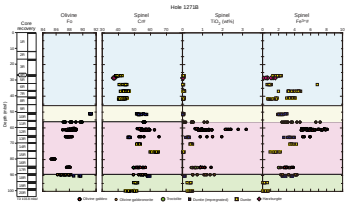

F11. Compositional variations of spinel, Hole 1271B, p. 20.

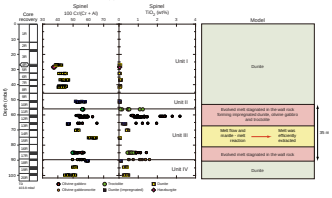

low Mg#. Gabbroic material associated with the large volume of dunite indicates that the melt activity was significant in this region relative to other sites drilled during Leg 209 near the 15°20′ Fracture Zone.

Cannat et al. (1997) reported coarse-grained gabbroic dikelets in harzburgite from Site 920 in the Kane Fracture Zone (MARK) area near the Mid-Atlantic Ridge. These dikelets were considered to be cumulates or trapped melts from magmas that had undergone variable degrees of crystal fractionation and differentiation before crystallizing in the ultramafic rocks. Most dikelets are <1 cm thick; rare dikelets are >5 cm thick. A 3.5-cm-thick gabbroic dike contains spinel with Mg# = 46.8, Cr# = 49.9, and TiO_2 = 1.4 wt%, similar to spinel in olivine gabbro from Hole 1271B.

The association of olivine gabbro and troctolite with dunite also resembles those reported from Hess Deep Site 895 (Arai and Matsukage, 1996; Dick and Natland, 1996). Cannat et al. (1990) also reported similar lithologies from the Garret transform fault. The difference between Hess Deep Site 895 and Hole 1271B is that gabbroic material intruded into harzburgite in the former but into dunite in the latter. Hole 1271B dunite may have formed by dissolution of orthopyroxene in harzburgite by pervasive melt flow prior to the growth of hybrid rocks as a mixture of melt and dunite within a melt flow channel located in Unit III. The occurrence of similar lithologies in both fast-spreading and slow-spreading ridges may indicate that they followed a similar cooling path in the uppermost mantle.

The dunite associated with gabbroic material recovered in Hole 1271B is similar to the Mohorovicic (Moho) transition zone of ophiolite (Boudier and Nicolas, 1995; Koga et al., 2001). The Moho transition zone of the Oman ophiolite is dominantly composed of dunite with gabbros, pyroxenites, and chromitites showing evidence of intense magmatic activity such as diffuse melt impregnations and formation of dikes and sills (Boudier and Nicolas, 1995). Dunites in Hole 1271B are also inferred to have originally formed by extensive interaction with melt in the uppermost mantle. Melt pervasively percolated through the peridotite matrix in the early stage, and as temperature decreased the melt crystallized plagioclase and clinopyroxene. Finally, the evolved melt stagnated in the peridotite matrix and formed gabbroic materials (olivine gabbro, olivine gabbronorite, and troctolite).

The Cr# of spinel is commonly restricted to <60 in abyssal peridotites (Dick and Bullen, 1984; Arai, 1987). However, the Cr# of spinel in Hole 1271B dunite reaches a maximum value of 62.7 at the center of Unit III. The formation of such high-Cr# spinel may be due to preferential extraction of the $MgAl_2O_4$ component from spinel during dissolution by migrating melt. Moreover, dunite with high-Cr# spinel is in contact with hybrid rocks in the upper and lower horizons. We interpret the occurrence of refractory dunite and hybrid rocks in Unit III to indicate that a large melt channel is located in Unit III. In the center of the melt channel the dunite became more refractory due to partial dissolution of spinel, whereas in the wall rock the melt lost heat and crystallized plagioclase and clinopyroxene. The melt evolved by fractional crystallization was finally trapped in the dunite matrix, forming hybrid rocks. The width of Unit III may indicate the scale of the melt flow channel in the uppermost mantle. Because of possible tectonic rotation of peridotite and the lack of constraints on the relative position of drilling the hole, the true thickness of the melt channel is ambiguous. In any case, the interval of Unit III may indicate that the maximum width of melt channel was ~35 m.

ACKNOWLEDGMENTS

We thank the *JOIDES Resolution* shipboard and technical staff for their help during cruise. Discussions with Peter Kelemen, Eiichi Kikawa, Anna Cipriani, Henry Dick, Ulrich Faul, Carlos Garrido, and the Leg 209 Scientific Party were very helpful in preparing manuscript. E.T. thanks Sumio Miyashita and Toshiaki Shimura for assistance with electron microprobe analysis. The manuscript was improved by comments from Cin-Ty Lee and the Publication Services Department of the Integrated Ocean Drilling Program.

This research used samples and/or data provided by the Ocean Drilling Program (ODP). ODP is sponsored by the U.S. National Science Foundation and participating countries under management of Joint Oceanographic Institutions (JOI), Inc. This research was supported by Japan Society for the Promotion of Science (numbers 16540413 and 11204101 to E.T.).

REFERENCES

Arai, S., 1987. An estimation of the least depleted spinel peridotite on the basis of olivine-spinel mantle array. *Neues Jahrb. Mineral. Monatsh.,* 8:347–354.

Arai, S., 1994. Characterization of spinel peridotites by olivine-spinel compositional relationships: review and interpretation. *Chem. Geol.,* 113(3–4):191–204. **doi:10.1016/0009-2541(94)90066-3**

Arai, S., and Matsukage, K., 1996. Petrology of the gabbro-troctolite-peridotite complex from Hess Deep, equatorial Pacific: implications for mantle-melt interaction within the oceanic lithosphere. *In* Mével, C., Gillis, K.M., Allan, J.F., and Meyer, P.S. (Eds.), *Proc. ODP, Sci. Results,* 147: College Station, TX (Ocean Drilling Program), 135–155. **doi:10.2973/odp.proc.sr.147.008.1996**

Boudier, F., and Nicolas, A., 1995. Nature of the Moho Transition Zone in the Oman ophiolite. *J. Petrol.,* 36:777–796.

Cannat, M., 1996. How thick is the magmatic crust at slow spreading oceanic ridges? *J. Geophys. Res.,* 101(B2):2847–2858. **doi:10.1029/95JB03116**

Cannat, M., Bideau, D., and Hébert, R., 1990. Plastic deformation and magmatic impregnation in serpentinized ultramafic rocks from the Garrett transform fault (East Pacific Rise). *Earth Planet. Sci. Lett.,* 101(2–4):216–232. **doi:10.1016/0012-821X(90)90155-Q**

Cannat, M., Chatin, F., Whitechurch, H., and Ceuleneer, G., 1997. Gabbroic rocks trapped in the upper mantle at the Mid-Atlantic Ridge. *In* Karson, J.A., Cannat, M., Miller, D.J., and Elthon, D. (Eds.), *Proc. ODP, Sci. Results,* 153: College Station, TX (Ocean Drilling Program), 243–264. **doi:10.2973/odp.proc.sr.153.013.1997**

Cannat, M., Mével, C., Maia, M., Deplus, C., Durand, C., Gente, P., Agrinier, P., Belarouchi, A., Dubuisson, G., Humler, E., and Reynolds, J., 1995. Thin crust, ultramafic exposures, and rugged faulting patterns at the Mid-Atlantic Ridge (22°–24°N). *Geology,* 23(1):49–52. **doi:10.1130/0091-7613(1995)023<0049:TCUEAR>2.3.CO;2**

Dick, H.J.B., 1989. Abyssal peridotites, very slow spreading ridges and ocean ridge magmatism. *In* Saunders, A.D., and Norry, M.J. (Eds.), *Magmatism in the Ocean Basins*. Geol. Soc. Spec. Publ., 42:71–105.

Dick, H.J.B., and Bullen, T., 1984. Chromian spinel as a petrogenetic indicator in abyssal and alpine-type peridotites and spatially associated lavas. *Contrib. Mineral. Petrol.,* 86(1):54–76. **doi:10.1007/BF00373711**

Dick, H.J.B., and Natland, J.H., 1996. Late-stage melt evolution and transport in the shallow mantle beneath the East Pacific Rise. *In* Mével, C., Gillis, K.M., Allan, J.F., and Meyer, P.S. (Eds), *Proc. ODP, Sci. Results,* 147: College Station, TX (Ocean Drilling Program), 103–134. **doi:10.2973/odp.proc.sr.147.007.1996**

Fujiwara, T., Lin, J., Matsumoto, T., Kelemen, P.B., Tucholke, B.E., and Casey, J.F., 2003. Crustal evolution of the Mid-Atlantic Ridge near the Fifteen-Twenty Fracture Zone in the last 5 Ma. *Geochem., Geophys., Geosyst.,* 4(3):1024. **doi:10.1029/2002GC000364**

Irvine, T.N., 1965. Chromium spinel as a petrogenetic indicator, Part 1. Theory. *Can. J. Earth Sci.,* 2:648–672.

Irvine, T.N., 1967. Chromium spinel as a petrogenetic indicator, Part 2. Petrological applications. *Can. J. Earth Sci.,* 4:71–103.

Kelemen, P.B., 1990. Reaction between ultramafic rock and fractionating basaltic magma, I. Phase relations, the origin of calc-alkaline magma series, and the formation of discordant dunite. *J. Petrol.,* 31:51–98.

Kelemen, P.B., Hirth, G., Shimizu, N., Spiegelman, M., and Dick, H.J.B., 1997. A review of melt migration processes in the asthenospheric mantle beneath oceanic spreading centers. *Philos. Trans. R. Soc. London, Ser. A,* 355:283–318.

Kelemen, P.B., Kikawa, E., Miller, D.J., et al., 2004. *Proc. ODP, Init. Repts.,* 209: College Station, TX (Ocean Drilling Program). **doi.10.2973/odp.proc.ir.209.2004**

Koga, K.T., Kelemen, P.B., and Shimizu, N., 2001. Petrogenesis of the crust-mantle transition zone and the origin of lower crustal wehrlite in the Oman ophiolite. *Geochem., Geophys., Geosyst.,* 2(9). **doi:10.1029/2000GC000132**

Quick, J.E., 1981. The origin and significance of large, tabular dunite bodies in the Trinity peridotite, northern California. *Contrib. Mineral. Petrol.,* 78:413–422.

Seyler, M., Lorand, J.-P., Dick, H.J.B., and Drouin, M., 2007. Pervasive melt percolation reactions in ultra-depleted refractory harzburgites at the Mid-Atlantic Ridge, 15°20′: ODP Hole 1274A. *Contrib., Mineral., Petrol.,* 153 (3):303–319. **doi:10.1007/s00410-006-0148-6**

Figure F1. Location of drilling sites for ODP Leg 209 indicated on the shaded relief bathymetry from multibeam survey of the Mid-Atlantic Ridge in the vicinity of the 15°20′ Fracture Zone (FZ) (modified after Fujiwara et al., 2003).

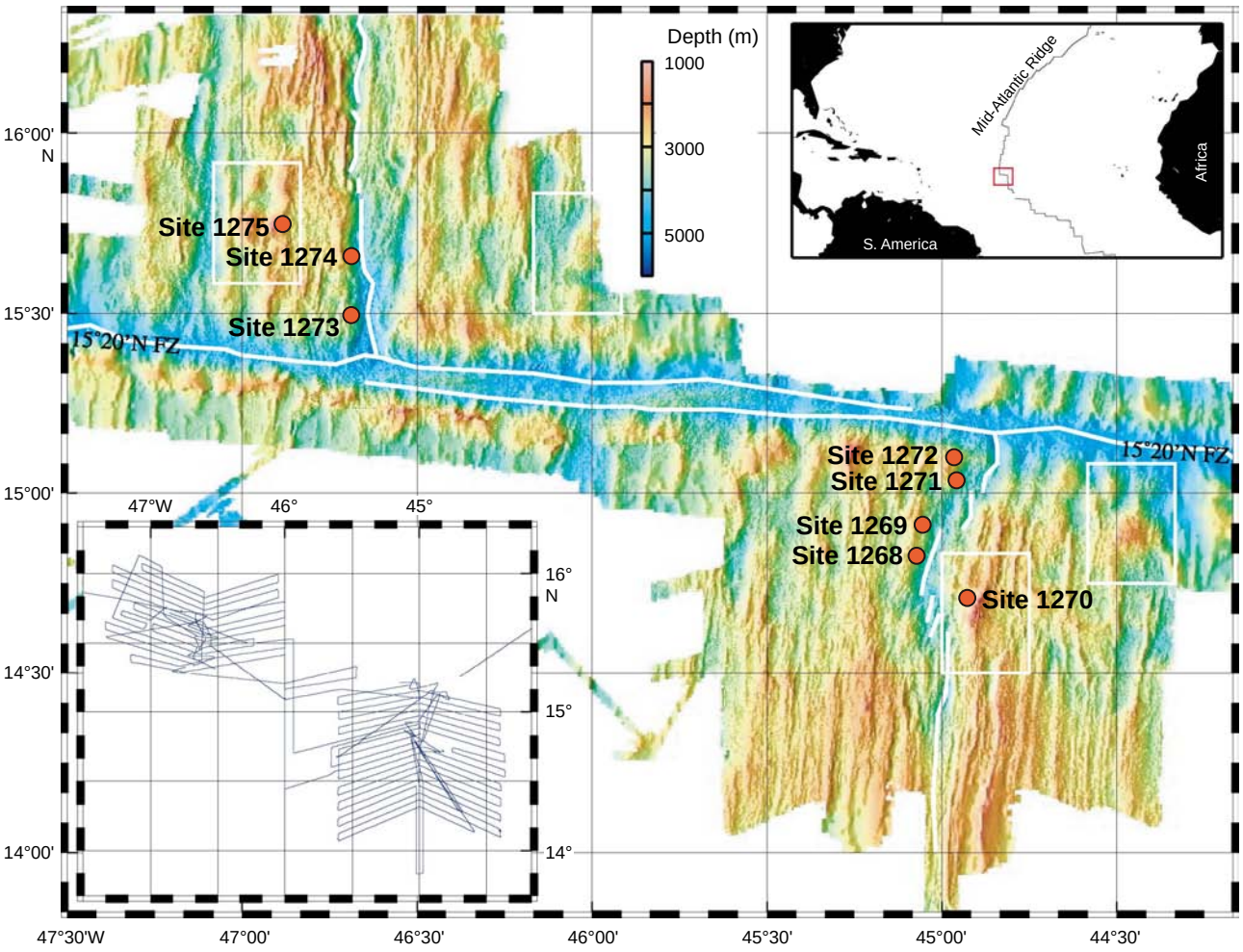

Figure F2. Lithostratigraphic summary for Hole 1271B. TD = total depth. D/H = dunite/harzburgite.

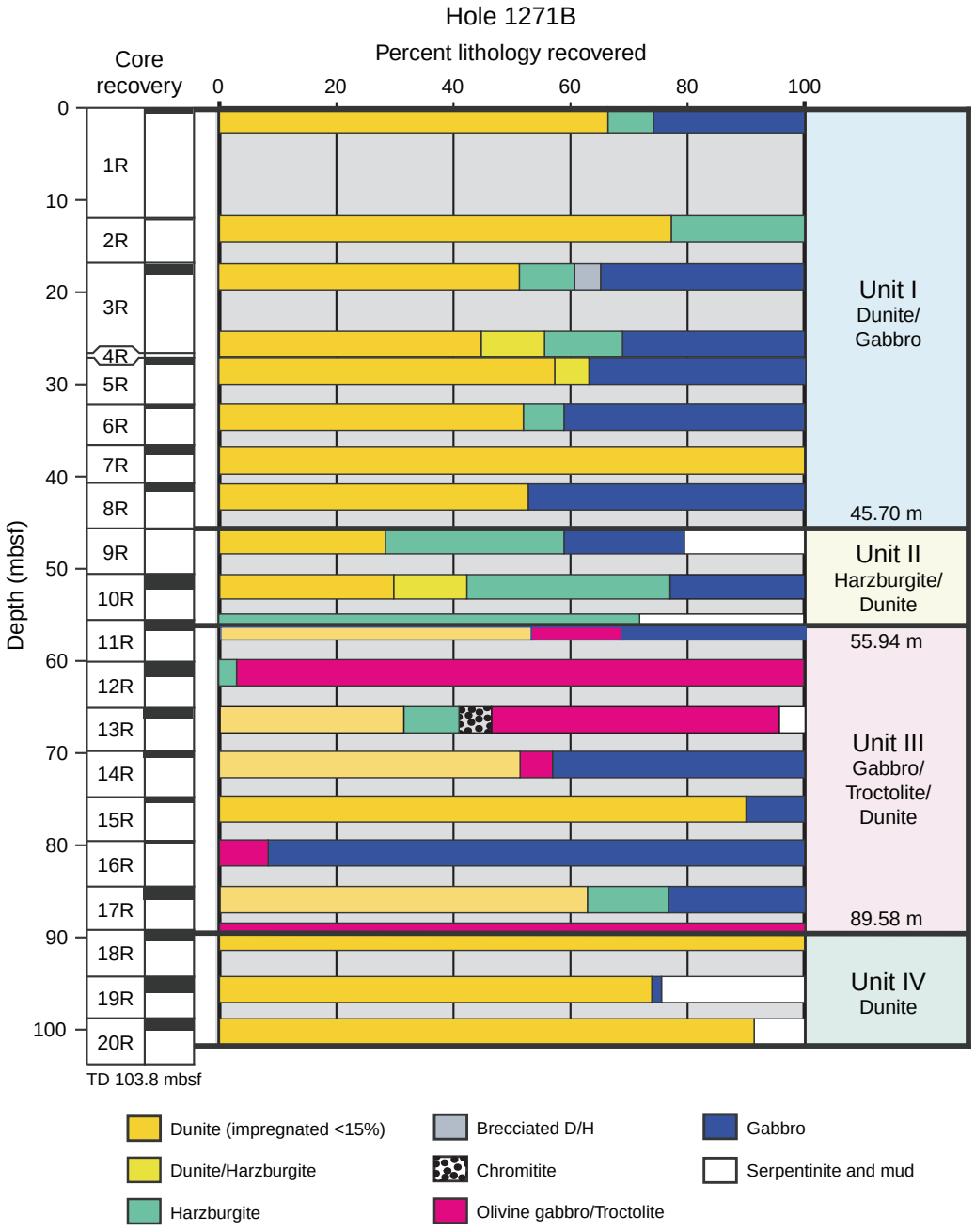

Figure F3. Spinel grains (circled). **A.** Sample 209-1271B-4R-1 (Piece 6, 28–31 cm) (reflected light; Cr# = 38.2). **B.** Sample 209-1271B-7R-1 (Piece 7, 49–54 cm) (Cr# = 45.1). **C, D.** Sample 209-1271B-10R-1 (Piece 15, 82–84 cm) (Cr# = 52.7); (C) reflected light; (D) plane-polarized light. **E.** Sample 209-1271B-12R-1 (Piece 12, 68–72 cm) (reflected light; Cr# = 57–59). **F.** Sample 209-1271B-15R-1 (Piece 5, 23–26 cm) (reflected light; Cr# = 64.0). Scale bar = 1mm.

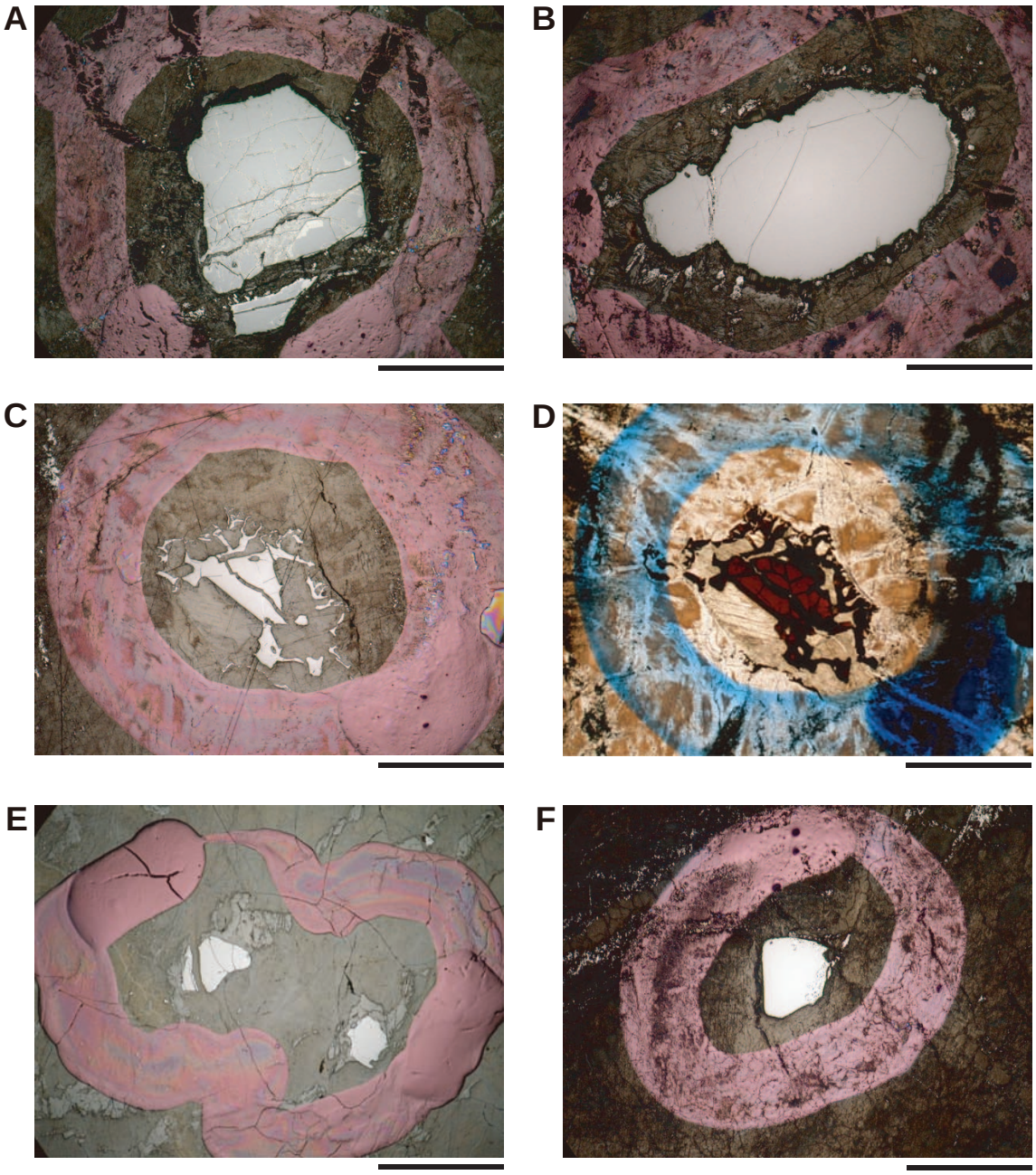

Figure F4. Histogram of forsterite molecular percent in olivines from Holes 1271B, 1272A, and 1274A.

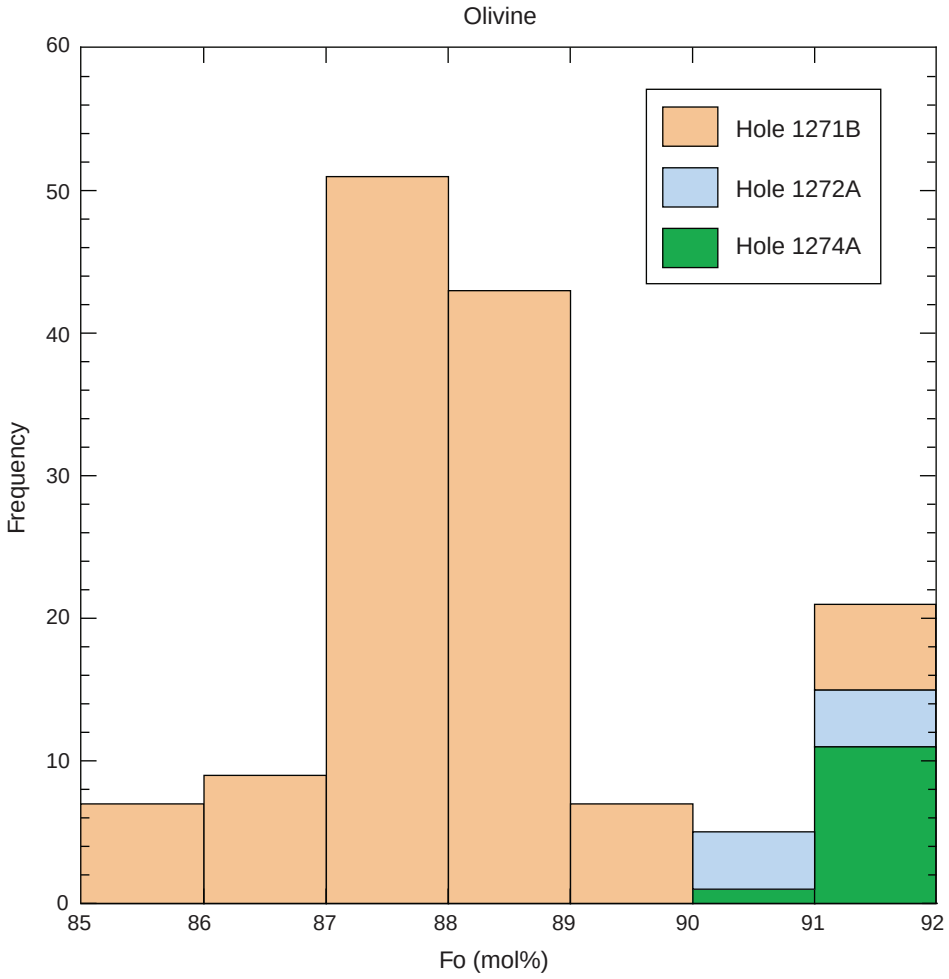

Figure F5. Compositions of Hole 1271B spinels plotted on the Cr-Al-Mg-Fe^{2+} face of the spinel composition prism (Irvine, 1965, 1967). Molecular Cr × 100/(Cr + Al) ratio of spinel is plotted against Mg × 100/(Mg + Fe^{2+}) ratio. Compositional fields for Hess Deep Site 895 spinel (East Pacific Rise) and abyssal chromites from Dick and Natland (1996) and Dick and Bullen (1984), respectively.

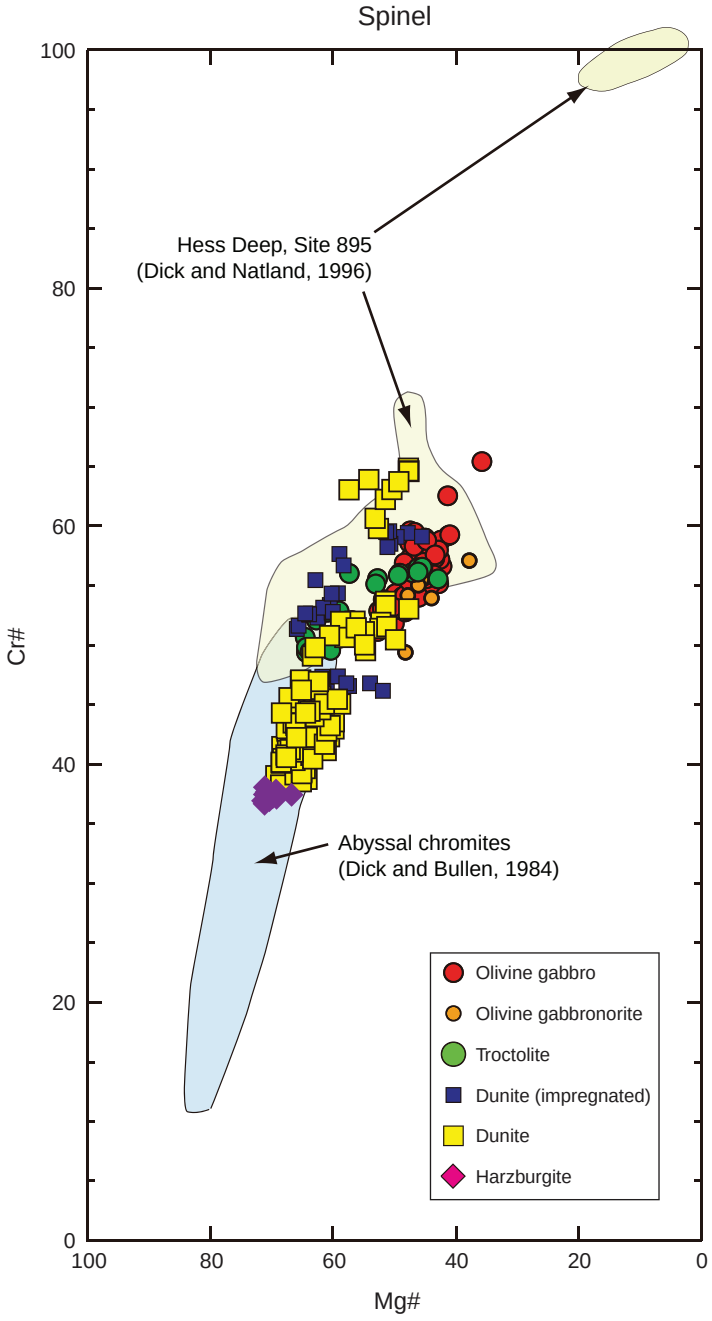

Figure F6. TiO_2 vs. molecular Cr × 100/(Cr + Al) ratio (Cr#) for spinel in Hole 1271B. Two trends are shown by arrows. Along the first trend ("Reaction 1"), Cr# increases while TiO_2 remains very low. In the second trend ("Reaction 2"), both TiO_2 and Cr# increase as the amount of gabbroic material increases in order from dunite through troctolite to olivine gabbro and olivine gabbronorite. This second trend is very similar to that for spinel at Hess Deep Site 895 (Arai and Matsukage, 1996). EPR = East Pacific Rise.

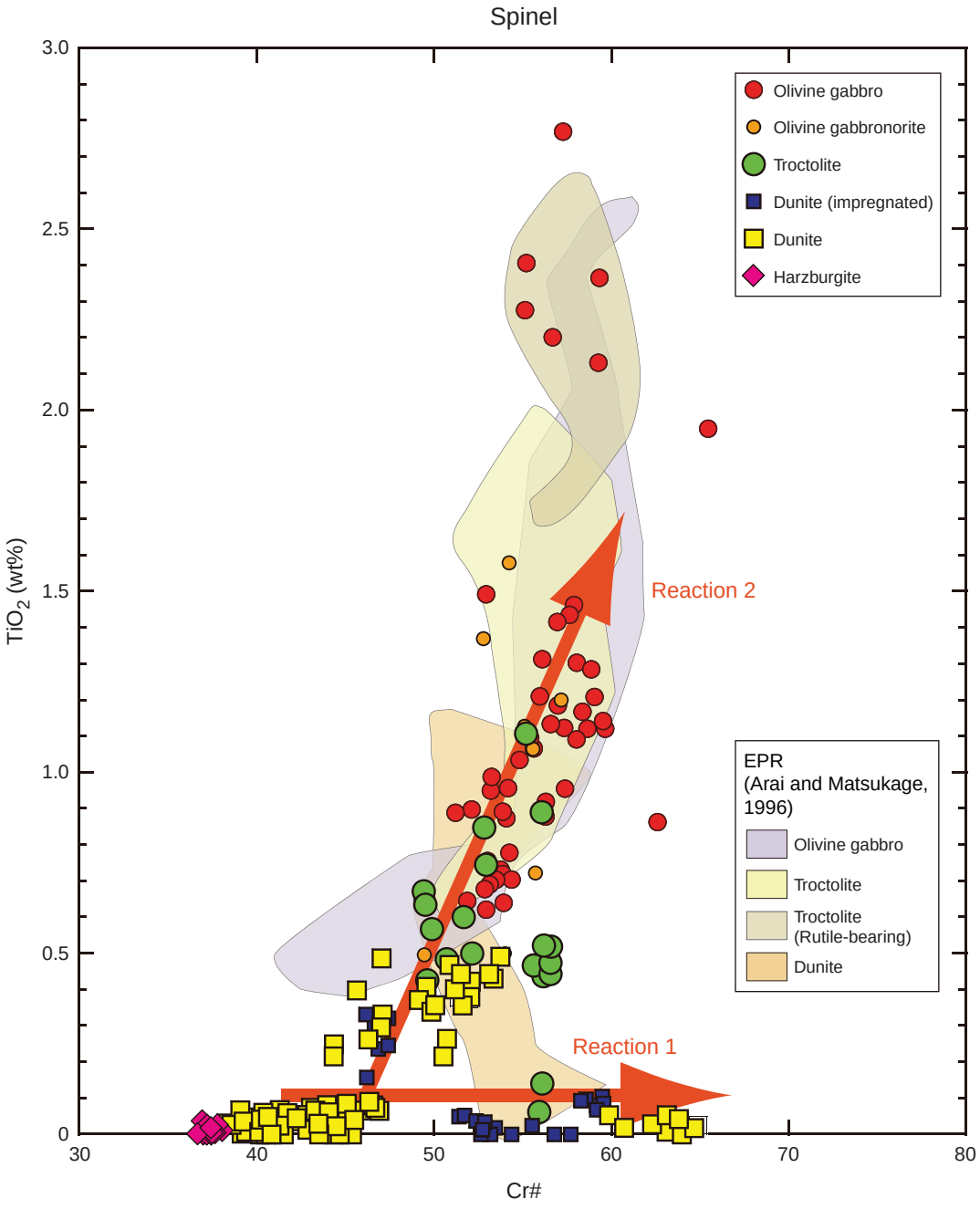

Figure F7. TiO_2 vs. molecular $Fe^{3+} \times 100/(Cr + Al + Fe^{3+})$ ratio (Fe#) for spinel in Hole 1271B. As in Figure F6, p. 15, two trends are distinguished.

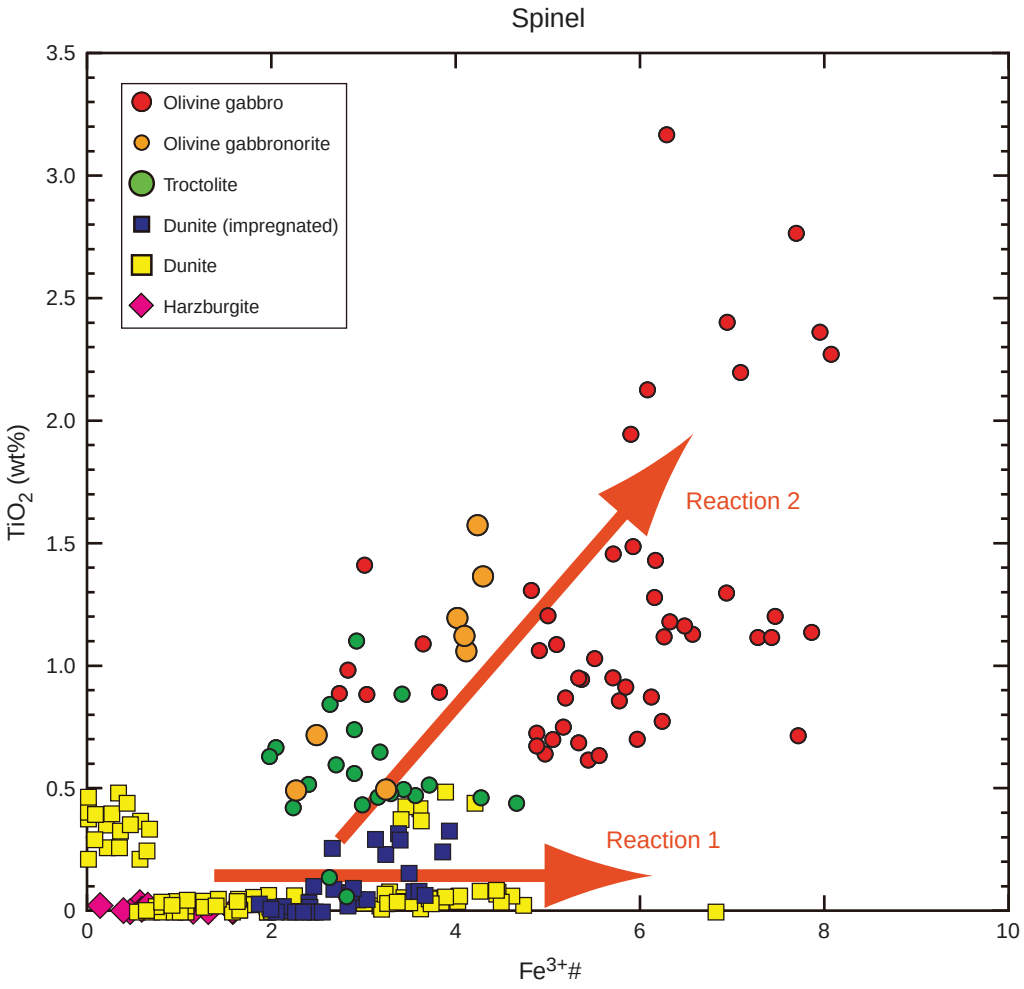

Figure F8. Relationship between Cr × 100/(Cr + Al) ratio (Cr#) of spinel and Fo of coexisting olivine in Holes 1271B, 1272A, and 1274A. The region labeled by OSMA indicates olivine-spinel mantle array of Arai (1994). Compositional fields for spinel at Hess Deep Site 895 are from Arai and Matsukage (1996). EPR = East Pacific Rise.

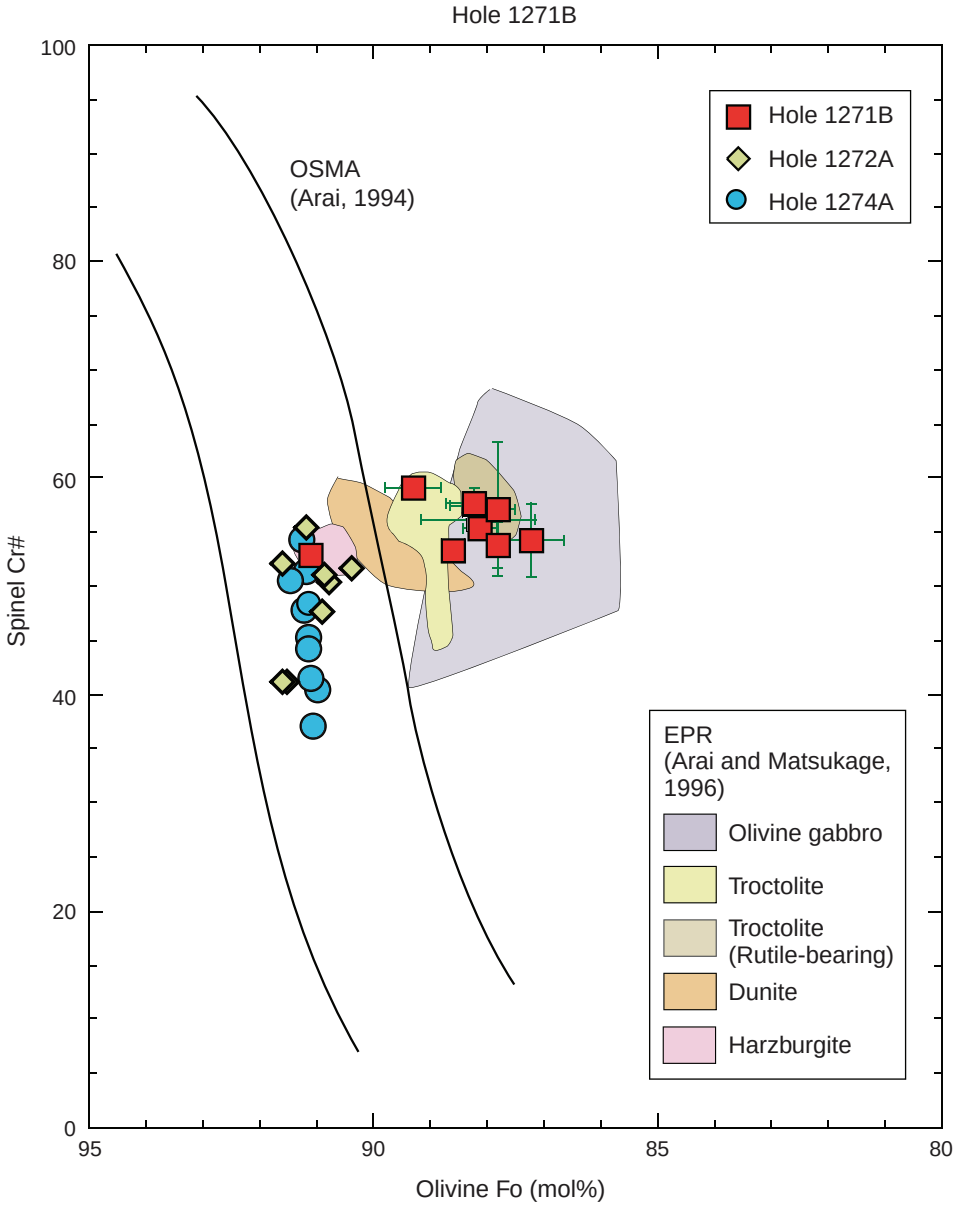

Figure F9. Ca amphibole compositions in olivine gabbro, troctolite, and brown amphibole gabbro plotted on Na + K vs. Si (atoms per formula unit). Tr = tremolite, Hb = hornblende, Ts = tschermakite, Ed = edenite, Pa = pargasite. BAG = brown amphibole gabbro.

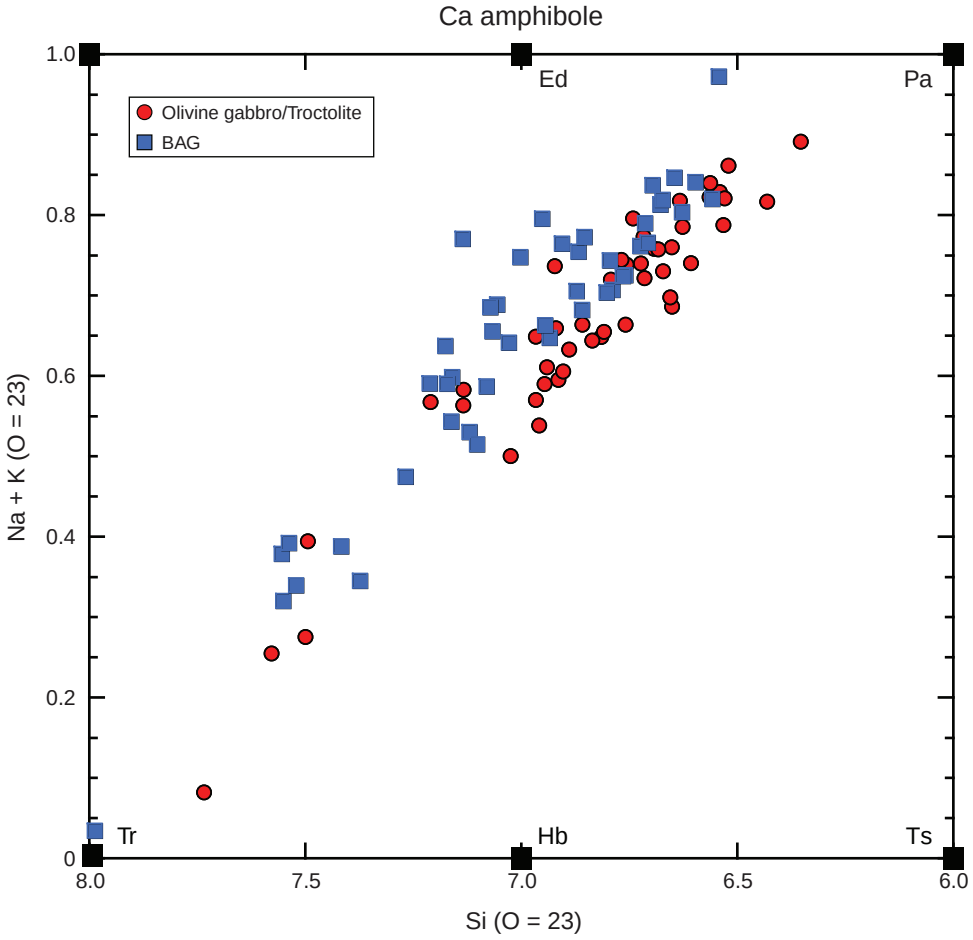

Figure F10. Downhole compositional variations of olivine and spinel. See text for detail. TD = total depth.

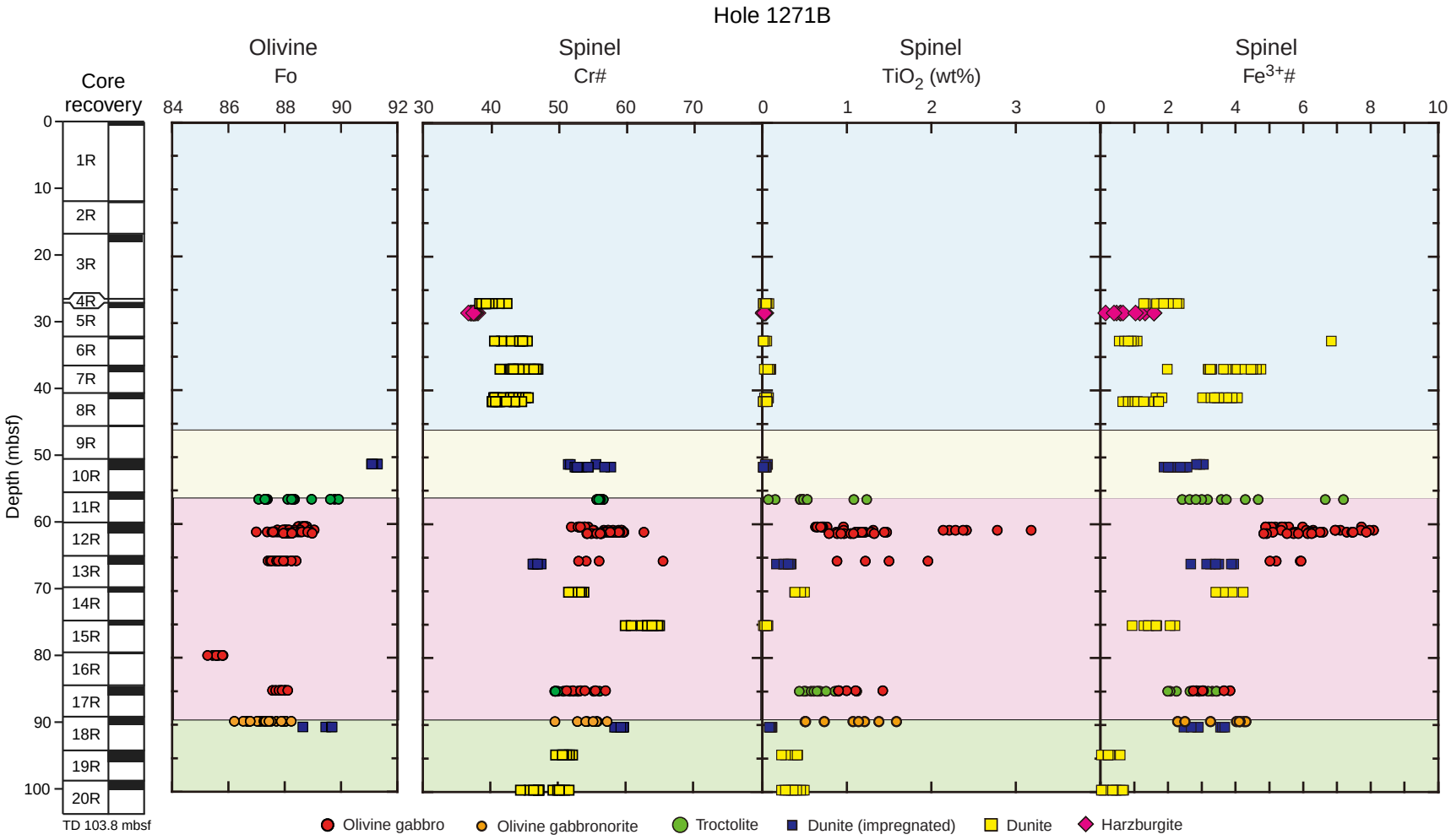

Figure F11. A schematic model interpreting downhole compositional variations of spinel in Hole 1271B. A melt channel is recognized in Unit III where hybrid rocks formed by stagnation of evolved melt resulted in impregnated dunite, troctolite and olivine gabbro/gabbronorite. TD = total depth.

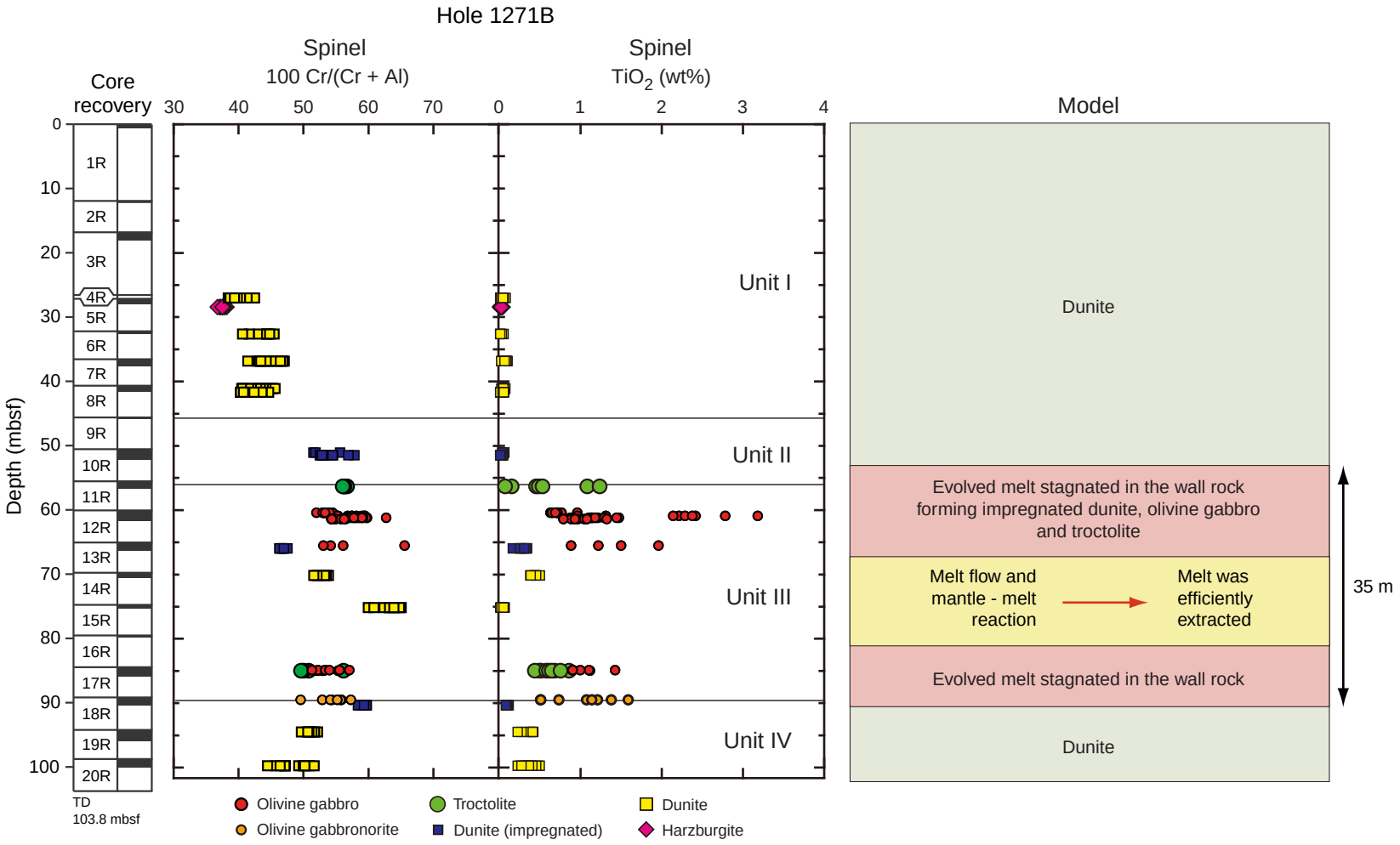

Table T1. Olivine composition, Hole 1271B.

Core, section	Interval (cm)	Depth (mbsf)	*N*	SiO_2	TiO_2	Al_2O_3	Cr_2O_3	FeO	MnO	NiO	MgO	CaO	Total	Fo
209-1271B-														
Dunite (impregnated)														
10R-1	43–46	50.93	4	41.4	0.01	0.00	0.02	8.7	0.11	0.30	50.4	0.09	101.1	91.2
			SD	0.3	0.01	0.00	0.02	0.1	0.05	0.02	0.2	0.02	0.2	0.1
18R-1	110–113	90.2	4	41.6	0.03	0.00	0.01	10.5	0.12	0.35	48.8	0.03	101.5	89.2
			SD	0.1	0.02	0.00	0.01	0.4	0.02	0.05	0.7	0.03	0.2	0.5
Troctolite														
11R-1	70–75	56.2	14	40.9	0.02	0.00	0.03	11.5	0.12	0.34	48.3	0.01	101.3	88.2
			SD	0.2	0.02	0.00	0.04	0.9	0.02	0.06	0.8	0.01	0.3	1.0
Olivine gabbro														
12R-1	17–22	60.27	5	40.8	0.00	0.00	0.02	11.1	0.14	0.26	48.6	0.03	101.0	88.6
			SD	0.7	0.01	0.00	0.03	0.1	0.04	0.05	0.4	0.02	1.0	0.1
12R-1	68–72	60.78	10	40.7	0.00	0.00	0.01	11.4	0.12	0.28	48.1	0.02	100.7	88.3
			SD	0.2	0.01	0.00	0.02	0.4	0.05	0.08	0.3	0.01	0.5	0.4
12R-1	96–99	61.06	4	40.6	0.02	0.00	0.01	11.4	0.18	0.30	48.7	0.03	101.3	88.4
			SD	0.1	0.02	0.01	0.01	0.5	0.07	0.09	0.4	0.01	0.3	0.5
12R-1	115–120	61.25	10	40.7	0.01	0.00	0.02	11.5	0.16	0.28	48.2	0.02	100.9	88.2
			SD	0.2	0.01	0.00	0.02	0.3	0.03	0.03	0.4	0.02	0.6	0.3
13R-1	27–30	65.37	15	40.1	0.01	0.01	0.03	11.8	0.14	0.31	47.8	0.02	100.3	87.8
			SD	0.5	0.02	0.01	0.02	0.3	0.05	0.07	0.4	0.02	0.8	0.3
16R-1	3–8	79.53	7	40.4	0.01	0.01	0.01	13.9	0.14	0.16	46.3	0.04	101.0	85.6
			SD	0.3	0.01	0.01	0.03	0.2	0.09	0.05	0.2	0.02	0.5	0.2
17R-1	22–25	84.72	8	41.3	0.00	0.01	0.02	11.8	0.17	0.26	47.9	0.06	101.5	87.8
			SD	0.2	0.01	0.01	0.02	0.2	0.02	0.06	0.4	0.02	0.5	0.2
Olivine gabbronorite														
18R-1	27–30	89.37	7	40.1	0.03	0.00	0.03	11.6	0.13	0.21	47.3	0.06	99.5	87.9
			SD	0.2	0.03	0.01	0.04	0.3	0.06	0.06	0.2	0.03	0.6	0.2

Notes: *N* = number of analyses making up the averaged composition. Fo = Mg × 100/(Mg + Fe); SD = one standard deviation.

Table T2. Spinel compositions, Hole 1271B.

Core, section	Interval (cm)	Depth (mbsf)	*N*	SiO_2	TiO_2	Al_2O_3	Cr_2O_3	Fe_2O_3	FeO	MnO	MgO	CaO	NiO	Total	Cr#	Mg#	Fe^{3+}#
209-1271B-																	
Harzburgite																	
5R1	64–67	28.34	6	0.02	0.02	37.4	33.3	0.43	12.4	0.18	16.6	0.01	0.12	100.5	37.4	70.4	0.5
			SD	0.01	0.01	0.4	0.3	0.18	0.3	0.06	0.2	0.01	0.05	0.4	0.5	0.8	0.2
Dunite																	
4R-1	28–31	26.88	7	0.04	0.02	35.3	33.6	1.58	14.1	0.17	15.1	0.00	0.33	100.3	38.9	65.7	1.7
			SD	0.04	0.01	0.4	0.3	0.31	0.5	0.03	0.4	0.01	0.03	0.5	0.4	1.4	0.3
6R-1	30–33	32.5	5	0.07	0.00	33.0	37.1	0.73	14.0	0.19	15.1	0.00	0.21	100.5	43.0	65.8	0.8
			SD	0.02	0.01	1.5	1.3	0.19	0.8	0.03	0.7	0.00	0.03	0.9	1.9	2.4	0.2
7R-1	49–54	36.69	13	0.07	0.05	30.9	36.5	3.30	13.8	0.21	15.0	0.00	0.11	100.0	44.2	65.9	3.7
			SD	0.02	0.02	1.3	0.7	0.64	0.5	0.04	0.4	0.00	0.05	0.3	1.5	1.4	0.8
8R-1	28–31	40.98	8	0.09	0.04	31.6	36.0	3.26	15.5	0.22	14.1	0.01	0.14	101.0	43.3	61.8	3.6
			SD	0.07	0.01	1.1	1.5	0.21	0.6	0.04	0.4	0.01	0.03	0.6	1.9	1.6	0.2
8R-1	83–87	41.53	6	0.06	0.02	34.2	35.0	0.93	13.2	0.19	15.6	0.01	0.10	99.4	40.7	67.7	1.0
			SD	0.02	0.02	0.4	0.3	0.29	0.3	0.04	0.2	0.01	0.05	0.6	0.5	0.8	0.3
14R-1	20–24	70	4	0.09	0.40	25.5	41.5	3.04	18.5	0.21	11.8	0.01	0.09	101.1	52.2	53.2	3.5
			SD	0.04	0.03	0.4	0.7	0.09	0.9	0.03	0.5	0.01	0.05	0.6	0.8	2.2	0.1
15R-1	23–26	75.03	2	0.06	0.02	19.5	48.8	1.37	18.5	0.22	10.6	0.00	0.04	99.1	62.7	50.6	1.6
			SD	0.02	0.00	1.7	1.5	0.45	1.3	0.02	0.9	0.00	0.05	0.7	2.8	3.9	0.6
19R-1	25–28	94.35	5	0.06	0.33	27.0	41.6	0.07	17.6	0.19	12.1	0.01	0.10	99.2	50.8	55.2	0.1
			SD	0.03	0.09	0.4	0.9	0.20	1.3	0.04	0.8	0.01	0.09	0.4	0.9	3.5	0.2
20R-1	81–84	99.61	10	0.06	0.35	29.6	39.8	0.28	14.5	0.20	14.4	0.02	0.06	99.2	47.4	63.9	0.3
			SD	0.01	0.09	1.8	1.5	0.22	1.3	0.04	1.1	0.03	0.06	0.4	2.4	3.8	0.2
Dunite (impregnated)																	
10R-1	43–46	50.93	2	0.14	0.05	26.7	42.3	2.64	13.7	0.23	14.8	0.00	0.15	100.6	51.5	65.8	3.0
			SD	0.00	0.00	0.3	0.1	0.05	0.0	0.03	0.1	0.00	0.03	0.4	0.2	0.2	0.1
10R-1	82–84	51.32	13	0.02	0.01	25.4	43.9	1.95	15.1	0.23	13.6	0.01	0.06	100.3	53.7	61.5	2.2
			SD	0.02	0.01	1.2	1.0	0.19	0.7	0.03	0.6	0.01	0.03	0.6	1.7	2.1	0.2
13R-1	70–73	65.8	6	0.12	0.28	29.1	38.4	2.90	16.5	0.23	13.4	0.01	0.13	101.1	46.9	59.0	3.3
			SD	0.06	0.03	0.3	0.4	0.35	1.2	0.04	0.8	0.01	0.09	0.5	0.4	3.3	0.4
18R-1	110–113	90.2	6	0.10	0.09	21.5	46.4	2.55	19.0	0.25	10.8	0.01	0.12	100.9	59.1	50.3	3.0
			SD	0.03	0.01	0.4	0.4	0.41	0.5	0.04	0.3	0.01	0.04	0.5	0.6	1.3	0.5
Troctolite																	
11R-1	70–75	56.2	5	0.02	0.34	22.7	43.4	2.52	20.0	0.28	10.1	0.00	0.07	99.4	56.3	47.2	3.0
			SD	0.02	0.22	0.4	0.4	0.48	0.8	0.04	0.4	0.00	0.04	0.3	0.3	2.0	0.6
17R-1	32–35	84.82	8	0.03	0.69	26.0	40.9	2.39	15.0	0.21	13.9	0.00	0.17	99.3	51.3	62.3	2.8
			SD	0.02	0.14	1.7	1.3	0.45	1.0	0.05	0.7	0.01	0.07	0.4	2.4	2.8	0.5
Olivine gabbro																	
12R-1	17–22	60.27	7	0.04	0.68	23.8	40.3	4.49	19.2	0.26	11.0	0.01	0.08	99.8	53.2	50.4	5.3
			SD	0.02	0.05	0.5	0.5	0.29	0.6	0.03	0.4	0.01	0.03	0.5	0.8	1.6	0.3
12R-1	68–72	60.78	5	0.09	2.29	19.5	39.6	5.46	22.3	0.26	9.3	0.00	0.17	99.0	57.6	42.7	7.0
			SD	0.03	0.67	1.0	1.1	0.47	0.7	0.03	0.3	0.01	0.09	0.4	1.7	1.2	0.6
12R-1	96–99	61.06	4	0.03	1.22	20.8	42.0	5.21	20.7	0.31	10.1	0.01	0.09	100.4	57.5	46.6	6.4
			SD	0.01	0.15	0.4	0.7	0.18	0.8	0.07	0.5	0.02	0.06	0.7	0.7	2.1	0.2
12R-1	115–120	61.25	6	0.09	0.98	22.1	40.7	4.67	20.4	0.26	10.2	0.00	0.09	99.4	55.3	47.1	5.7
			SD	0.05	0.18	0.6	0.7	0.44	0.6	0.03	0.3	0.01	0.02	0.4	1.0	1.4	0.5
13R-1	27–30	65.37	4	0.04	1.03	22.5	41.3	2.93	21.3	0.27	9.5	0.01	0.11	99.0	55.2	44.3	3.6
			SD	0.08	0.46	3.4	2.7	0.33	2.0	0.05	1.5	0.00	0.07	0.4	5.7	6.2	0.5
17R-1	22–25	84.72	5	0.16	1.06	23.7	42.0	2.68	19.4	0.25	11.4	0.01	0.09	100.7	54.3	51.1	3.2
			SD	0.08	0.22	1.5	0.7	0.43	1.2	0.03	1.0	0.01	0.04	0.9	1.9	3.7	0.5
Olivine gabbronorite																	
18R-1	27–30	89.37	5	0.04	1.03	22.5	41.3	2.93	21.3	0.27	9.5	0.01	0.11	99.0	46.3	65.2	0.3
			SD	0.01	0.42	0.8	1.0	0.58	1.3	0.05	0.9	0.01	0.07	0.6	1.3	3.8	0.7

Notes: *N* = number of analyses making up the average composition. Cr# = (Cr × 100)/(Cr + Al); Mg# = (Mg × 100)/(Mg + Fe^{2+}); Fe^{3+}# = (Fe^{3+} × 100)/(Al + Cr + Fe^{3+}); SD = one standard deviation.

Table T3. Amphibole composition, Hole 1271B.

Core, section	Interval (cm)	Depth (mbsf)	*N*	SiO_2	TiO_2	Al_2O_3	Cr_2O_3	FeO	MnO	MgO	NiO	CaO	Na_2O	K_2O	Total	Mg#	Si	Na + K
209-1271B-																		
Dunite																		
7R-1	49–54	36.69	1	45.5	0.31	11.9	2.40	2.91	0.07	19.0	0.05	12.6	2.98	0.00	97.6	0.921	6.43	0.82
Troctolite																		
11R-1	70–75	56.2	3	52.4	0.22	6.0	0.93	3.10	0.06	21.0	0.10	11.9	1.89	0.04	97.7	0.923	7.28	0.52
			SD	1.8	0.05	1.5	0.43	0.20	0.03	0.7	0.05	0.4	0.38	0.01	0.6	0.007	0.19	0.10
12R-1	17–22	60.27	3	47.7	0.17	10.4	1.32	3.61	0.10	19.7	0.12	11.9	2.83	0.07	97.8	0.907	6.70	0.79
			SD	1.9	0.12	2.1	0.08	0.21	0.03	0.9	0.04	0.3	0.15	0.00	0.8	0.009	0.20	0.05
Olivine gabbro																		
12R-1	68–72	60.78	2	46.6	0.08	11.2	1.48	3.88	0.03	19.2	0.10	11.8	2.95	0.07	97.4	0.898	6.60	0.82
			SD	0.5	0.04	0.7	0.24	0.17	0.01	0.2	0.03	0.2	0.01	0.01	0.4	0.005	0.05	0.00
12R-1	115–120	61.25	1	47.4	0.04	11.0	0.87	3.97	0.13	19.2	0.04	12.0	2.73	0.08	97.5	0.896	6.69	0.76
13R-1	27–30	65.37	1	47.9	0.23	9.5	1.20	3.84	0.14	19.9	0.16	11.7	2.66	0.09	97.3	0.902	6.77	0.75
16R-1	3–8	79.53	3	49.6	0.73	8.6	0.30	4.66	0.10	19.4	0.02	12.2	2.32	0.10	98.0	0.881	6.95	0.65
			SD	1.4	0.44	1.5	0.44	0.31	0.06	0.7	0.04	0.1	0.26	0.04	0.1	0.010	0.17	0.08
Brown amphibole gabbro																		
3R-1	34–39	17.25	12	53.5	1.37	5.34	0.03	4.33	0.08	21.1	0.06	11.8	1.69	0.03	99.3	0.897	7.08	0.45
			SD	1.78	0.41	1.95	0.03	0.46	0.03	0.56	0.05	0.21	0.36	0.02	0.3	0.010	0.21	0.10
3R-1	84–90	17.85	16	49.9	2.30	7.65	0.01	4.38	0.07	19.2	0.10	11.5	2.47	0.06	97.7	0.887	7.00	0.68
			SD	2.7	0.89	2.16	0.01	0.60	0.03	1.2	0.05	0.2	0.55	0.02	0.6	0.020	0.31	0.16
4R-1	21–24	26.81	13	51.0	1.49	6.72	0.05	4.24	0.07	20.2	0.09	11.6	1.94	0.04	97.5	0.894	7.14	0.53
			SD	3.1	0.83	3.10	0.06	0.38	0.04	0.8	0.04	0.4	0.76	0.02	0.4	0.009	0.38	0.21
4R-1	69–72	27.29	11	48.6	2.68	8.17	0.04	5.41	0.09	18.5	0.08	11.7	2.80	0.06	98.2	0.859	6.84	0.77
			SD	1.3	0.79	1.18	0.05	0.37	0.04	0.3	0.03	0.4	0.17	0.01	0.5	0.008	0.18	0.05
14R-1	8–10	69.88	5	49.9	1.90	6.67	0.02	6.85	0.11	18.2	0.13	11.7	1.98	0.04	97.6	0.826	7.08	0.55
			SD	2.0	0.68	1.53	0.03	0.54	0.02	0.9	0.03	0.3	0.57	0.02	0.3	0.018	0.25	0.16

Notes: Depth is based on expanding the curated recovery to fill the drilled interval. *N* = number of analyses making up averaged compositions; Mg# = Mg/(Mg + Fe); Si = molecular Si on 23 oxygens; Na + K = molecular Na and K on 23 oxygens; SD = one standard deviation.